Fluctuations and All-In–All-Out Ordering in Dipole-Octupole $Nd_2Zr_2O_7$

E. Lhotel,[1,*] S. Petit,[2,†] S. Guitteny,[2] O. Florea,[1] M. Ciomaga Hatnean,[3] C. Colin,[1,5] E. Ressouche,[4] M. R. Lees,[3] and G. Balakrishnan[3]

[1]*CNRS, Institut NEEL, F-38000 Grenoble, France*
[2]*Laboratoire Léon Brillouin, CEA-CNRS UMR 12, CE-Saclay, F-91191 Gif-sur-Yvette, France*
[3]*Department of Physics, University of Warwick, Coventry, CV4 7AL, United Kingdom*
[4]*INAC SPSMS, CEA and Université Joseph Fourier, F-38000 Grenoble, France*
[5]*Univ. Grenoble Alpes, Institut NEEL, F-38000 Grenoble, France*

(Received 3 July 2015; published 4 November 2015)

By means of neutron scattering and magnetization measurements down to 90 mK, we determine the magnetic ground state of the spin-ice candidate $Nd_2Zr_2O_7$. We show that, despite ferromagnetic interactions, $Nd_2Zr_2O_7$ undergoes a transition around 285 mK towards an all-in–all-out antiferromagnetic state, with a strongly reduced ordered magnetic moment. We establish the (H, T) phase diagram in the three directions of the applied field and reveal a metamagnetic transition around 0.1 T, associated with an unexpected shape of the magnetization curves. We propose that this behavior results from the peculiar nature of the Nd^{3+} doublet, a dipolar-octupolar doublet, different from the standard Kramers doublet studied to date, thus revealing the importance of multipolar correlations in the properties of pyrochlore oxides.

DOI: 10.1103/PhysRevLett.115.197202 PACS numbers: 75.10.Jm, 75.25.-j, 75.40.-s, 75.50.Ee

Understanding, characterizing, and classifying novel states of matter is one of the main issues of research in frustrated systems [1,2]. Much of the recent activity in this field has focused on $4f$ pyrochlores. Here, the frustration arises from the lattice, built from tetrahedra connected by their corners. The situation where the magnetic moments on these vertices are coupled via a ferromagnetic nearest-neighbor interaction and constrained by the crystal electric field (CEF) anisotropy to lie along local $\langle 111 \rangle$ axes has received a lot of attention, as it leads classically to a macroscopically degenerated ground state, where each tetrahedron has two spins pointing in and two spins pointing out, called "spin ice" [3,4]. The quest for the quantum variant of spin ice (QSI) has attracted further strong interest. A wealth of fascinating phenomena, like the emergence of gauge fields along with unconventional excitations, are expected [5]. Such QSI systems remain to be explored experimentally. Compounds with a positive Curie-Weiss temperature θ_{CW} indicative of ferromagnetic interactions, along with a strong Ising-like anisotropy, are, *a priori*, possible QSI candidates. In this Letter, we focus on $Nd_2Zr_2O_7$, which falls into this class, as shown by magnetization [6–8] and CEF studies [8,9].

$Nd_2Zr_2O_7$ stands out as a fascinating system because of an additional interesting property. The Nd^{3+} crystal field ground doublet, represented as a pseudospin $1/2$, is a Kramers doublet called a "dipolar-octupolar" (DO) doublet, and is different from the widely studied Kramers doublet as in $Er_2Ti_2O_7$ [10–12], $Er_2Sn_2O_7$ [13], or $Yb_2Ti_2O_7$ [14]: two components of the pseudospin $1/2$ transform like a magnetic dipole, while the other transforms like the component of the magnetic octupole tensor [15–18]. This results in a rich theoretical phase diagram: besides ordered phases like the all-in–all-out structure (AIAO) where dipoles point along the local axes toward or away from the tetrahedron centers, an antiferro-octupolar phase appears along with QSI phases [18].

In this Letter, we explore this physics by means of neutron and magnetization measurements down to very low temperature. Using inelastic neutron scattering, we first study the CEF excitations to shed light on the Ising and DO nature of the Nd^{3+} ground state doublet. Despite the fact that ferromagnetic interactions ($\theta_{CW} > 0$) should stabilize a spin-ice state, we then show that $Nd_2Zr_2O_7$ orders in an antiferromagnetic AIAO structure below $T_N = 285$ mK with a magnetic moment reduced by about two-thirds. This is related to the existence of unusually strong magnetic fluctuations in the ordered phase, which might result from the proximity of the expected spin-ice state. The AIAO state can be reproduced by mean-field calculations with an effective antiferromagnetic coupling that, however, contradicts $\theta_{CW} > 0$. The reduced ordered magnetic moment and the peculiar shape of the magnetization versus field curves can actually be accounted for by considering local fluctuations induced by octupolar correlations.

Magnetization and ac susceptibility measurements were performed in two SQUID magnetometers equipped with dilution refrigerators developed at the Institut Néel [19]. The experiments were carried out down to 90 mK on a powder sample and a parallelepiped single crystal of $Nd_2Zr_2O_7$ grown by the floating zone technique ($2.35 \times 1.72 \times 1.36$ mm^3) [20]. The magnetic field was applied along the three cubic high symmetry directions [100], [110], and [111]. Powder neutron diffraction experiments have been conducted on D1B (CNRS CRG–ILL, France) using a wavelength $\lambda = 2.52$ Å. We repeated the same

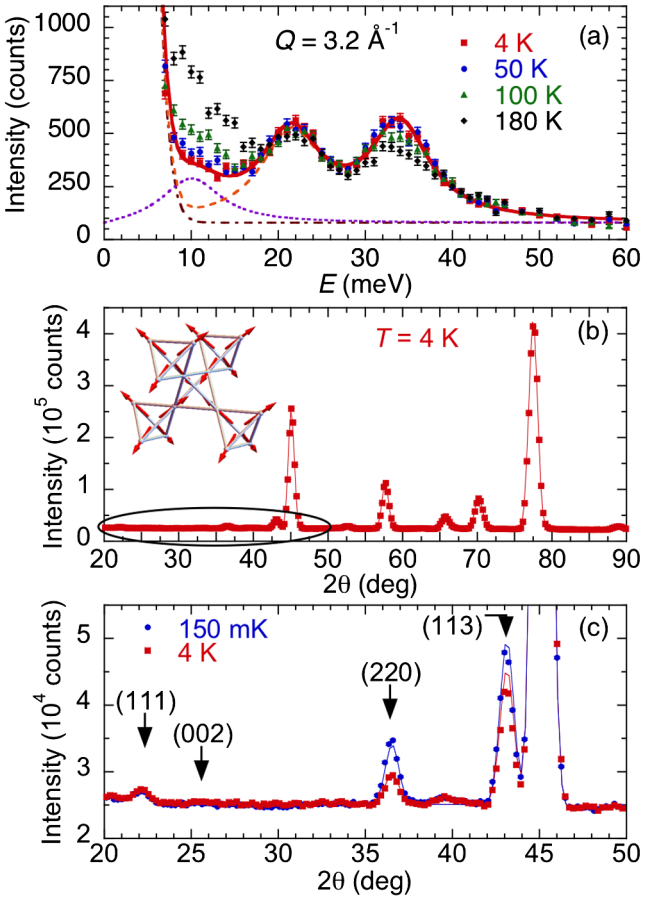

FIG. 1 (color online). (a) Inelastic neutron scattering spectra at $Q = 3.2$ Å^{-1} for several temperatures. The solid line is the sum of the fitted contributions at 4 K, including the elastic incoherent scattering tail (dot-dashed line), the phonon mode around 10 meV (dotted line), and CEF modes at 22 and 34 meV (dashed line) [21]. (b) Powder diffractogram at 4 K. The line is a fit to the $Fd\bar{3}m$ structure. Inset: Scheme of the AIAO state. (c) Zoom on the low angle part at 150 mK and 4 K showing the magnetic contribution. The lines are combined refinements of the crystallographic and magnetic structures.

experiment on 4F2 (LLB, France), using $\lambda = 2.36$ Å, with a second sample that was also used for macroscopic measurements, and measured the CEF excitations on this second sample by means of inelastic neutron scattering on the thermal triple axis spectrometer 2T (LLB). Single crystal diffraction experiments were carried out on D23 (CEA CRG–ILL) using $\lambda = 1.28$ and 2.4 Å.

First, we focus on the DO nature of the ground doublet in $Nd_2Zr_2O_7$ and study the CEF excitations. As shown in Fig. 1(a), the neutron intensity exhibits two clear peaks around 22 and 34 meV. The intensities of both excitations remain constant at larger wave vector Q and decrease slightly as the temperature increases. This temperature dependence provides evidence for the magnetic origin of both modes, which are thus attributed to two CEF transitions. At 10 meV, another contribution is clearly observed

TABLE I. Wybourne coefficients (in K), g factors, and ground state wave functions of Nd^{3+} in $Nd_2Zr_2O_7$ from inelastic neutron scattering analysis.

B_{20}	B_{40}	B_{43}	B_{60}	B_{63}	B_{66}	$g_\parallel$	$g_\perp$
−190	5910	110	2810	10	−890	4.5	0

J_z	−9/2	−7/2	−5/2	−3/2	±1/2	3/2	5/2	7/2	9/2
$\|\uparrow\rangle$	−0.878	0	0	−0.05	0	0.476	0	0	0.009
$\|\downarrow\rangle$	−0.009	0	0	0.476	0	0.05	0	0	−0.878

in data with a better energy resolution. The strong increase in the intensity of this feature with increasing temperature and wave vector is typical of a phonon mode (See Supplemental Material [21]). The energy of the two CEF modes match the theoretical analysis based on macroscopic measurements, which takes into account the mixing of the $^4I_{9/2}$ and $^4I_{11/2}$ multiplets of the $4f^3$ Nd^{3+} ion's electronic configuration [8]. Note that the theory predicts two distinct modes around 32 meV that could not be resolved in the experiment [22]. To explicitely show the DO character of the doublet, and determine wave functions that are easier to handle, we consider the CEF Hamiltonian within the ground multiplet $^4I_{9/2}$ only: $\mathcal{H}_{\mathrm{CEF}} = \sum_{m,n} B_{nm} O_{nm}$, where the O_{nm} are the Wybourne operators ($J = 9/2$, $g_J = 8/11$) [23]. The B_{nm} coefficients are refined by fitting the crystal field contribution of the neutron data (energy levels and intensities) along with the value of the local magnetic moment at low temperature $2.3\mu_B$ [see Fig. 1(a) and Table I]. This analysis confirms the above mentioned theory [8], yielding the picture of very strong Ising Nd^{3+} moments with $g_\perp \equiv 0$, $g_\parallel = 4.5$ and modes at 21.8, 33.5, 34.5, and 109 meV. The coefficients of the ground doublet wave functions $|\uparrow, \downarrow\rangle$ (see Table I) are similar to the ones found in $Nd_2Ir_2O_7$ [16] and typical of a DO doublet [15,18].

Our magnetization and ac susceptibility measurements reveal a transition at low temperature, as expected from specific heat measurements [6]. The susceptibility exhibits a peak both in the real and imaginary parts at a temperature of 410 mK for the powder sample, consistent with Ref. [6] (data not shown), and at a lower temperature of 285 mK for the single crystal (see Fig. 2). Despite $\theta_{CW} > 0$ (see inset of Fig. 2), the shape of the χ' peak as well as its amplitude are characteristic of an antiferromagnetic transition. The position of the peak does not depend on frequency (in the measured range $f = 0.11$–570 Hz). However, as the frequency increases, the peak in χ'' lies on top of a background below 4 K, which increases with decreasing temperature (data not shown), similarly to what was observed in $Tb_2Ti_2O_7$ [24]. This observation might be the signature of slow fluctuations, which are not affected by the antiferromagnetic transition.

This antiferromagnetic transition is further confirmed by neutron diffraction measurements, on both powder and

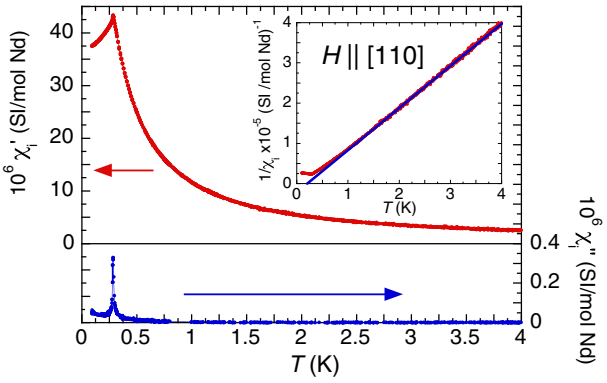

FIG. 2 (color online). ac susceptibility χ_i' and χ_i'' versus temperature T along [110] with $\mu_0 H_{ac} = 0.27$ mT and $f = 5.7$ Hz, corrected for demagnetization effects. Inset: $1/\chi_i'$ versus T. The line is a fit between 1 and 4 K to the Curie-Weiss law $1/\chi = (2.05 \times 10^4) - (1.05 \times 10^5)T$, giving $\theta_{CW} = (195 \pm 15)$ mK and an effective moment $\mu_{\text{eff}} = (2.45 \pm 0.02)\,\mu_B$.

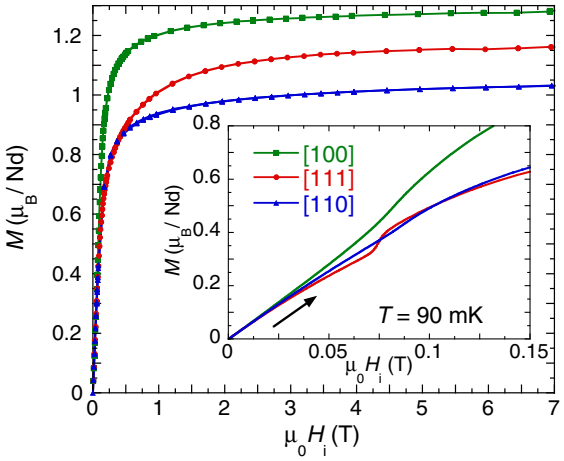

FIG. 3 (color online). Magnetization M versus internal field H_i measured along the three main directions at 90 mK. Inset: Detailed view of the low field data. The field was swept up from negative to positive values.

single crystal samples. At 4 K [see Fig. 1(b)], the powder FULLPROF refinement [25] in the $Fd\bar{3}m$ space group yields a lattice parameter $a = 10.66$ Å and the O2 oxygen position $x = 0.335$ (with a RF factor of 2). The magnetic contribution rises below T_N superimposed on the nuclear Bragg peaks, revealing that the propagation vector of the magnetic structure is $\mathbf{k} = (0, 0, 0)$ [see Fig. 1(c)]. Consequently, from symmetry analysis, the representation of the magnetic structure involves four irreducible representations $\Gamma_{3,5,7,9}$ [26], which correspond to the four different magnetic structures compatible with the $Fd\bar{3}m$ group symmetry. Γ_3 corresponds to the AIAO structure [see inset of Fig. 1(b)] predicted for multiaxis Ising pyrochlore antiferromagnets [27], Γ_5 to the structure of the antiferromagnetic XY pyrochlore magnet $Er_2Ti_2O_7$ [28], Γ_7 to the structure of dipolar pyrochlore magnets such as $Gd_2Sn_2O_7$ [29,30], and Γ_9 to the splayed ferromagnetic $Yb_2Sn_2O_7$ structure [30,31]. Given the second-order nature of the transition, the magnetic structure is described by only one of these representations. The FULLPROF refinement of the diffractogram [see Fig. 1(c)] shows that the AIAO magnetic configuration (Γ_3 representation) is the only one that is compatible with the neutron data (R factor ≈8). Note that Γ_3 is the sole configuration that leads to zero magnetic intensity of the (111) and (002) (plus symmetry related) Bragg peaks, as observed in the experiment [see Fig. 1(c)]. The refinement yields a weak magnetic moment $m = (0.8 \pm 0.05)\mu_B$ indicating large fluctuations even at temperatures of about $T_N/4$.

We emphasize that this antiferromagnetic state, dressed with fluctuations, while $\theta_{CW} > 0$, is the signature of an unconventional ground state, emerging from the inherent frustration of the system. It is worth mentioning that, although classically expected in multiaxis Ising pyrochlore antiferromagnets [27], the AIAO state has only been observed in systems (such as FeF_3 [32], $Cd_2Os_2O_7$ [33], $Na_3Co(CO_3)_2Cl$ [34] and pyrochlore iridates [35,36]) where additional ingredients have to be involved in the Hamiltonian. Actually, it has never been reported in pyrochlore compounds with $3d$ transition metal, making $Nd_2Zr_2O_7$ a peculiar case in this family.

M versus H measurements were performed in order to determine the (H, T) phase diagram of the system. Down to 90 mK, the saturated magnetization depends on the field direction (see Fig. 3). The obtained values are, within 10%, those expected for magnetic moments with a multiaxis Ising anisotropy [37] and correspond to a total magnetic moment $m \approx 2.3\mu_B$, consistent with the effective moment of the Curie-Weiss law (see inset of Fig. 2). This shows that, although the ordered moment is reduced in the AIAO phase, the total magnetic moment is recovered in high magnetic fields, and remains with a strong Ising character. At low field, the slope of the magnetization curves is not zero (see inset of Fig. 3), contrary to what is expected for such an Ising system in an AIAO state. This confirms that a part of the magnetic moment is still fluctuating at low temperature. An inflexion point is present in these curves around 0.1 T, which can be attributed to a metamagnetic process towards the field-induced ordered phase. It is observed in the three directions of the applied field, but is more pronounced along the [111] direction. The temperature dependence of this metamagnetic process can be followed by plotting the derivative dM/dH_i of the magnetization curve (see inset of Fig. 4). Assuming that the maximum of dM/dH_i corresponds to the metamagnetic field value, we plot the phase diagram as a function of temperature (see Fig. 4). As expected, the peak in dM/dH_i disappears at the transition temperature. The obtained phase diagram is almost isotropic, and the data can be fitted to a $T - T_N$ law which gives an exponent slightly larger than $1/2$.

We now compare these experimental results with mean-field calculations. To this end, we consider a model taking

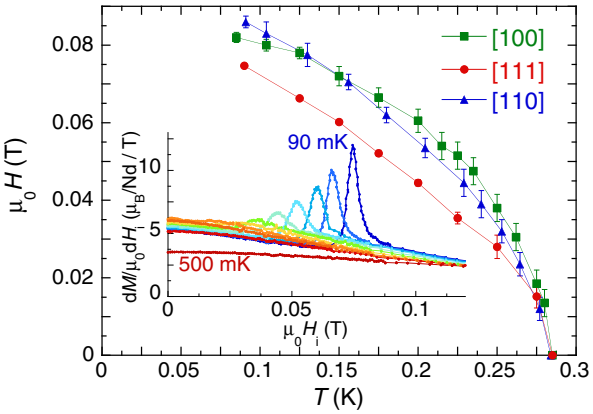

FIG. 4 (color online). (H, T) phase diagram obtained from the maximum of dM/dH_i versus H_i. Inset: dM/dH_i versus H_i in the [111] direction.

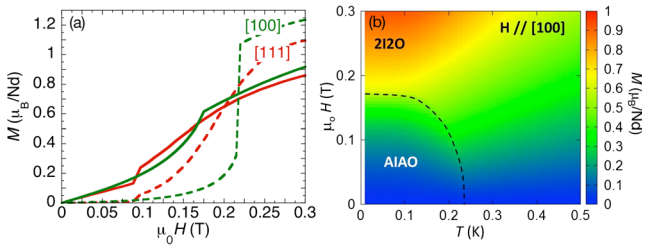

FIG. 5 (color online). (a) Calculated M versus H at $T = 100$ mK with $J^z = -5$ mK for $H \parallel [100]$ (green) and [111] (red). Full (dashed) lines are calculated with $U/|\alpha| = 2.7$ mK (0 K), with $\alpha \approx 73i$ from Table I. (b) Color plot of $M(H, T)$ for $J^z = -5$ mK and $U/|\alpha| = 2.7$ mK. The dashed line shows the transition boundary.

into account $\mathcal{H}_{\mathrm{CEF}}$ and a unique coupling J^z acting between nearest-neighbor local z components of the Nd^{3+} moments. An antiferromagnetic $J^z \sim -5$ mK allows us to reproduce the Néel temperature of about 300 mK and the AIAO structure. This leads to a (H, T) phase diagram similar to the experimental one, with a metamagneticlike transition from the AIAO state to the field-induced ordered state (3 in–1 out or 2 in–2 out, depending on the direction of the field). Nevertheless, this mean-field model fails to reproduce the positive θ_{CW} as well as the small amplitude of the ordered moment. In addition, the calculated field-induced transition is abrupt, corresponding to spin flips in the whole magnetic structure, in contrast to the smooth measured curves [see dashed lines in Fig. 5(a)].

These results support the existence of strong fluctuations which prevent a total ordering of the moment. From the coefficients of the DO wave function, $\langle\uparrow|J|\downarrow\rangle \equiv 0$, so the dipolar exchange alone cannot induce any on-site fluctuation from one element of the doublet to the other. Such fluctuations arise by virtue of the octupolar operator $\mathcal{T} = i(J^+J^+J^+ - J^-J^-J^-)$ [18], which, projected onto the subspace spanned by $|\uparrow\downarrow\rangle$, is written as $\mathcal{T} = \{\alpha|\uparrow\rangle\langle\downarrow| + \alpha^*|\downarrow\rangle\langle\uparrow|\}$ with $\alpha = \langle\uparrow|\mathcal{T}|\downarrow\rangle \neq 0$. This suggests that an octupole-octupole coupling, $\mathcal{V} \propto \sum_{\langle i,j\rangle} \mathcal{T}_i \mathcal{T}_j$, is at play. In the first instance, we can consider the approximate local form $\mathcal{V}' = \sum_i (U/|\alpha|)\mathcal{T}_i$, where U plays the role of an octupolar field. This induces a mixing that tends to bind the two elements of the doublet to form new states with reduced moments. In this picture, applying a magnetic field competes with $\mathcal{V}'$ and progressively unbinds $|\uparrow\rangle$ and $|\downarrow\rangle$. The effect of such a term is consistent with the experimental observations, since, as shown in Fig. 5, it does reduce the ordered moment, and makes the magnetization curves and field-induced transition smoother. However, the calculation of the susceptibility with this value of J^z and taking into account $\mathcal{V}'$ still cannot reproduce the sign of θ_{CW}.

This discrepancy might be understood in the context of the pseudospin 1/2 theory developed recently for DO doublets [18]. It is shown that despite a positive J^z (corresponding to a ferromagneticlike interaction in that local frame convention), the antiferromagnetic AIAO ground state is stabilized by a negative transverse term J^x in a large region of the theoretical phase diagram. But due to the peculiar nature of the ground state doublet, only J^z contributes to the Curie-Weiss temperature, leading to a positive θ_{CW}. Further analysis of spin waves would help to determine these coupling constants and serve as a test of this hypothesis.

It is worth noting that this contradiction might also be removed in the context of the recently proposed fragmentation theory [38]. In this model, for a certain range of microscopic parameters, the classical spin-ice phase can fragment into an AIAO antiferromagnetic phase with a reduced moment and a Coulomb phase characteristic of the spin-ice correlations. Such a scenario could be confirmed by diffuse scattering measurements, showing the coexistence of Bragg peaks and pinch points.

In summary, our inelastic neutron scattering results confirm the Ising and DO nature of the ground state doublet of the Nd^{3+} ion. We establish the existence of an antiferromagnetic AIAO ordering, although the ferromagnetic interactions should lead to a spin-ice state. However, strong fluctuations, unexpected in an Ising magnet, reduce the magnetic moment. These fluctuations are suppressed by a moderate magnetic field while the system undergoes a metamagnetic transition. This unusual set of observations can be understood by considering multipolar correlations that reintroduce quantum fluctuations in Ising systems. Indeed, in $Nd_2Zr_2O_7$, the DO nature of the doublet naturally calls for octupolar correlations. Further theoretical and experimental work is needed especially to determine the nature of magnetic excitations stemming from this peculiar ground state.

We thank C. Paulsen for allowing us to use his SQUID dilution magnetometers and V. Simonet, B. Canals,

R. Ballou, and B. Malkin for fruitful discussions. O. F. acknowledges a grant from the Laboratoire d'Excellence Laboratoire d'Alliances Nanosciences-Energies du Futur in Grenoble. M. C. H., M. R. L., and G. B. acknowledge financial support from the EPSRC, UK, Grant No. EP/M028771/1.

*elsa.lhotel@neel.cnrs.fr
†sylvain.petit@cea.fr

[1] *Introduction to Frustrated Magnetism*, edited by C. Lacroix, P. Mendels, and F. Mila (Springer-Verlag, Berlin, 2011).
[2] J. S. Gardner, M. J. P. Gingras, and J. E. Greedan, Rev. Mod. Phys. **82**, 53 (2010).
[3] M. J. Harris, S. T. Bramwell, D. F. McMorrow, T. Zeiske, and K. W. Godfrey, Phys. Rev. Lett. **79**, 2554 (1997).
[4] A. P. Ramirez, A. Hayashi, R. J. Cava, R. Siddharthan, and B. S. Shastry, Nature (London) **399**, 333 (1999).
[5] M. J. P. Gingras and P. A. McClarty, Rep. Prog. Phys. **77**, 056501 (2014).
[6] W. J. Blöte, R. F. Wielinga, and W. J. Huiskamp, Physica (Amsterdam) **43**, 549 (1969).
[7] K. Matsuhira, Y. Hinatsu, K. Tenya, H. Amitsuka, and T. Sakakibara, J. Phys. Soc. Jpn. **71**, 1576 (2002).
[8] M. C. Hatnean, M. R. Lees, O. A. Petrenko, D. S. Keeble, G. Balakrishnan, M. J. Gutmann, V. V. Klekovkina, and B. Z. Malkin, Phys. Rev. B **91**, 174416 (2015).
[9] S. Lutique, P. Javorsky, R. J. M. Konings, J.-C. Krupa, A. C. G. van Genderen, J. C. van Miltenburg, and F. Wastin, J. Chem. Thermodyn. **36**, 609 (2004).
[10] L. Savary, K. A. Ross, B. D. Gaulin, J. P. C. Ruff, and L. Balents, Phys. Rev. Lett. **109**, 167201 (2012).
[11] M. E. Zhitomirsky, M. V. Gvozdikova, P. C. W. Holdsworth, and R. Moessner, Phys. Rev. Lett. **109**, 077204 (2012).
[12] S. Petit, J. Robert, S. Guitteny, P. Bonville, C. Decorse, J. Ollivier, H. Mutka, M. J. P. Gingras, and I. Mirebeau, Phys. Rev. B **90**, 060410(R) (2014).
[13] S. Guitteny, S. Petit, E. Lhotel, J. Robert, P. Bonville, A. Forget, and I. Mirebeau, Phys. Rev. B **88**, 134408 (2013).
[14] K. A. Ross, L. Savary, B. D. Gaulin, and L. Balents, Phys. Rev. X **1**, 021002 (2011).
[15] A. Abragam and B. Bleaney, *Electron Paramagnetic Resonance of Transition Ions*, Oxford Classic Texts in the Physical Sciences (Oxford University Press, New York, 1970).
[16] M. Watahiki, K. Tomiyasu, K. Matsuhira, K. Iwasa, M. Yokoyama, S. Takagi, M. Wakeshima, and Y. Hinatsu, J. Phys. Conf. Ser. **320**, 012080 (2011).
[17] A. Bertin, Y. Chapuis, P. Dalmas de Réotier, and A. Yaouanc, J. Phys. Condens. Matter **24**, 256003 (2012).
[18] Y.-P. Huang, G. Chen, and M. Hermele, Phys. Rev. Lett. **112**, 167203 (2014).
[19] C. Paulsen, in *Introduction to Physical Techniques in Molecular Magnetism: Structural and Macroscopic Techniques–Yesa 1999*, edited by F. Palacio, E. Ressouche, and J. Schweizer (Servicio de Publicaciones de la Universidad de Zaragoza, Zaragoza, 2001), p. 1.
[20] M. Ciomaga Hatnean, M. R. Lees, and G. Balakrishnan, J. Cryst. Growth **418**, 1 (2015).
[21] See Supplemental Material at http://link.aps.org/supplemental/10.1103/PhysRevLett.115.197202 for the detailed analysis of inelastic scattering data, especially the temperature dependence of the phonon modes, as well as the Q dependence.
[22] An additional mode is predicted at 100 meV, but is not visible in the accessible energy range. Note that the observed CEF levels do not match those proposed in Ref. [9].
[23] B. G. Wybourne, *Spectroscopic Properties of Rare Earths* (Interscience, New York, 1965).
[24] E. Lhotel, C. Paulsen, P. D. de Réotier, A. Yaouanc, C. Marin, and S. Vanishri, Phys. Rev. B **86**, 020410(R) (2012).
[25] J. Rodríguez-Carvajal, Physica (Amsterdam) **192B**, 55 (1993); http://www.ill.eu/sites/fullprof/.
[26] A. Poole, A. S. Wills, and E. Lelièvre-Berna, J. Phys. Condens. Matter **19**, 452201 (2007).
[27] S. T. Bramwell and M. J. Harris, J. Phys. Condens. Matter **10**, L215 (1998).
[28] J. D. M. Champion, M. J. Harris, P. C. W. Holdsworth, A. S. Wills, G. Balakrishnan, S. T. Bramwell, E. Čižmár, T. Fennell, J. S. Gardner, J. Lago, D. F. McMorrow, M. Orendáč, A. Orendáčová, D. McK. Paul, R. I. Smith, M. T. F. Telling, and A. Wildes, Phys. Rev. B **68**, 020401(R) (2003).
[29] S. E. Palmer and J. T. Chalker, Phys. Rev. B **62**, 488 (2000).
[30] A. S. Wills, M. E. Zhitomirsky, B. Canals, J. P. Sanchez, P. Bonville, P. Dalmas de Réotier, and A. Yaouanc, J. Phys. Condens. Matter **18**, L37 (2006).
[31] A. Yaouanc, P. Dalmas de Réotier, P. Bonville, J. A. Hodges, V. Glazkov, L. Keller, V. Sikolenko, M. Bartkowiak, A. Amato, C. Baines, P. J. C. King, P. C. M. Gubbens, and A. Forget, Phys. Rev. Lett. **110**, 127207 (2013).
[32] G. Ferey, R. de Pape, M. Leblanc, and J. Pannetier, Rev. Chim. Miner. **23**, 474 (1986).
[33] J. Yamaura, K. Ohgushi, H. Ohsumi, T. Hasegawa, I. Yamauchi, K. Sugimoto, S. Takeshita, A. Tokuda, M. Takata, M. Udagawa, M. Takigawa, H. Harima, T. Arima, and Z. Hiroi, Phys. Rev. Lett. **108**, 247205 (2012).
[34] Z. Fu, Y. Zheng, Y. Xiao, S. Bedanta, A. Senyshyn, G. G. Simeoni, Y. Su, U. Rücker, P. Kögerler, and T. Brückel, Phys. Rev. B **87**, 214406 (2013).
[35] K. Tomiyasu, K. Matsuhira, K. Iwasa, M. Watahiki, S. Takagi, M. Wakeshima, Y. Hinatsu, M. Yokoyama, K. Ohoyama, and K. Yamada, J. Phys. Soc. Jpn. **81**, 034709 (2012).
[36] E. Lefrançois, V. Simonet, R. Ballou, E. Lhotel, A. Hadj-Azzem, S. Kodjikian, P. Lejay, P. Manuel, D. Khalyavin, and L. C. Chapon, Phys. Rev. Lett. **114**, 247202 (2015).
[37] M. J. Harris, S. T. Bramwell, P. C. W. Holdsworth, and J. D. M. Champion, Phys. Rev. Lett. **81**, 4496 (1998).
[38] M. E. Brooks-Bartlett, S. T. Banks, L. D. C. Jaubert, A. Harman-Clarke, and P. C. W. Holdsworth, Phys. Rev. X **4**, 011007 (2014).